Available online at www.sciencedirect.com

ScienceDirect

International Journal of Heat and Mass Transfer 50 (2007) 2346–2354

International Journal of HEAT and MASS TRANSFER

www.elsevier.com/locate/ijhmt

Effects of a finite section with linearly varying wall temperature on mixed convection in a vertical channel

Tsai-Shou Chang

Department of Power Mechanical Engineering, National Formosa University, 64 Wun-Hua Road, Huwei, Yuenlin 63208, Taiwan ROC

Received 27 July 2006; received in revised form 21 October 2006
Available online 28 December 2006

Abstract

Laminar mixed convection in a vertical channel with a finite section of a linearly varying wall temperature is numerically investigated. Dramatic variations of local velocity, temperature, local and average Nusselt numbers are plotted to demonstrate the influences of investigated parameters including Reynolds number, Grashof number and the degree of wall temperature variation. Particular attention is paid to reveal the effects of linearly varying temperature. The results suggest that the average Nusselt number $\overline{Nu}$ increases with Re and Gr. Moreover, $\overline{Nu}$ is higher with a linearly increasing wall temperature than that with a linearly decreasing wall temperature. Finally, an excellent correlation is proposed to predict $\overline{Nu}$ over the wide ranges of investigated parameters.

Keywords: Linearly varying wall temperature; Laminar mixed convection; Vertical channel

1. Introduction

Mixed convection flow through a heated channel has been extensively explored because of its occurrence in many practical applications such as the cooling of electronic equipment, heat exchangers, etc. Comprehensive reviews have been conducted by Incropera [1], Aung [2] and Gebhart et al. [3]. Most of the previous researches investigated the mixed convection with either uniform wall temperature or wall heat flux thermal boundary condition. However, these imposed thermal boundary conditions are not suitable in many practical applications such as heat exchangers [4,5], inject mold, transient setup and shutdown processes and non-equilibrium solidification processes. Furthermore, to meet the industrial requirements, a non-uniform thermal boundary is necessary. For example, Kim et al. [6] utilized a non-uniform temperature distribution to obtain a uniform thickness substance film in chemical deposition process. Therefore it is necessary to discover the influences of the non-uniform thermal boundary conditions on the heat transfer and flow characteristics in mixed convection flow. In the following, some of the published reports relevant to mixed convection and the effects of non-uniform thermal boundary are reviewed, respectively.

It is well known that buoyancy plays an important role on the forced fluid flow and heat transfer in a heated vertical channel. For an aiding flow with a sufficient high Gr/Re^2, the fluid near the heated walls is accelerated to a very high speed, causing the flow reversal in the central portion of the channel in order to maintain mass conservation. On the other hand, in general, a recirculating flow is observed near by the heated walls when the opposing buoyancy force is strong enough to reverse the forced flow locally. Consequently, understanding of mixed convection heat transfer becomes important and necessary. Tao [7] and Quintiere and Mueller [8] studied the steady fully developed and developing mixed convection. Habchi and Acharya [9] numerically investigated the aiding mixed convection of air. Their results show that the air temperature increases with Gr/Re^2 and the Nusselt number decreases monotonically. A similar study was performed by Aung and Worku

E-mail address: tschang@nfu.edu.tw

0017-9310/$ - see front matter
doi:10.1016/j.ijheatmasstransfer.2006.10.042

Nomenclature

b	channel spacing	T_m	mean temperature of the heated section
g	gravitational acceleration	u, v	dimensional velocities in x and y direction
Gr	Grashof number, $g\beta(T_m - T_e)b^3/v^2$	u_e	inlet velocity
h	convective heat transfer coefficient	$\overline{u}_e$	average inlet velocity
$\vec{i}, \vec{j}$	unit vector in X and Y direction, respectively	U, V	dimensionless velocities in X and Y direction
k	thermal conductivity of fluid	$\vec{V}^*$	provisional velocity vector
ℓ	length of the heated section	x, y	Cartesian coordinate
L	dimensionless length of the heated section	X, Y	dimensionless Cartesian coordinate
Nu	local Nusselt number		
$\overline{Nu}$	average Nusselt number	*Greek symbols*	
$\overline{Nu}_{cor}, \overline{Nu}_{num}$	$\overline{Nu}$ obtained from the proposed correlation and numerical simulation, respectively	α	thermal diffusivity
p	pressure	β	volumetric thermal expansion coefficient
P	dimensionless pressure, $(p - \rho g x)/\rho\overline{u}_e^2$	v	kinematic viscosity
Pr	Prandtl number	θ	dimensionless temperature, $\theta = (T - T_e)/(T_m - T_e)$
Re	Reynolds number, $\overline{u}_e b/v$	θ_1	dimensionless temperature at $X = 0$ and $Y = 0$
T	temperature	ρ	density of fluid
T_e	inlet temperature		

[10], indicating that buoyancy force can cause a severe distortion in the velocity profile especially under asymmetric heat condition. The mixed convection with a low Peclet number in a short channel was examined by Chow et al. [11]. Various axial length scales to distinguish regions of different convective mechanisms were discussed by Yao [12]. Cebeci et al. [13] investigated the recirculating flow and heat transfer in steady laminar opposing mixed convection in a vertical flat duct. Aung and Worku [14] and Lavine [15] proposed the criteria for the presence of reverse flow in vertical and inclined ducts, respectively. Ingham et al. [16,17] observed that poor heat transfer results for flow retarded by an opposing buoyancy force, but for a large and negative Gr/Re^2 heat transfer is rather effective. Actually, heat transfer may be greatly enhanced over the section containing a strong reverse flow.

It is a classical problem to consider the heat transfer of an infinite flat plate which has a power-law wall temperature distribution while the ambient being kept at a constant temperature [18]. Recently this problem has been re-investigated and combined with a few interesting features, for example, with a micropolar fluid [19], a thermally stratified porous medium [20], combined heat and mass transfer [21], linearly moving permeable surface [22] and MHD-free convection [23]. The effects of finite heating and/or cooling section are of interest, too. Effects of local cooling/heating surface in a thin vertical cylinder were studied by Kumari and Nath [24]. They assumed the variations of the wall temperature and wall heat flux are of the form, $(x - x_i)(x_j - x)/(x_j - x_i)^2$, where x is the axial coordinate and x_i, x_j are two pre-assigned positions. Ramos et al. [25] carried out the study on the effects of a sinusoidal wall temperature in an oscillatory flow. Their results show that the ambient velocity, the oscillatory frequency and the wave length of the sinusoidal wall temperature are the important parameters. Hernandez and Zamora [26] explored the effects of variable properties and non-uniform heating on the flow and heat behaviors in vertical channels. Particular attention is paid to the maximum mass flowrate in the channel inlet induced by natural convection when the wall heat flux was varied. Saeid and Yaacob [27] performed a computational work to study the influences of a sinusoidal side-wall temperature on the natural convection in a square cavity. They found that the imposed oscillatory amplitude and the wave number strongly affect the heat transfer. The maximum average Nusselt number occurs at a wave number about 0.7.

In addition to the spatial variation of thermal boundary conditions as reviewed above, it is also interested to consider the temporal variation. Turbulent channel flow with thermal stratification and wall temperature oscillation is studied numerically by Dong and Lu [28]. Large eddy simulation coupled with dynamic subgrid-scale models is employed to analysis the turbulent flow and heat transfer characteristics. The turbulent heat transfer is observed to be significantly affected by the forced wall temperature oscillation. The laminar mixed convection in an inclined channel was analytically investigated by Barletta and Zanchini [29]. Particular attention is focused on the effects resulted from the time-sinusoidal varying temperature distribution on the lower wall of the channel. A resonance frequency which corresponding to a maximum oscillatory amplitude of the Nusselt number is found for every Prandtl number. Malashetty and Basavaraja [30] examined the stability characteristics of a double diffusive convection in horizontal fluid layer by imposing symmetric or asymmetric temperature modulation on the top and bottom plates. Kwak et al. [31] investigate the effects of a time-dependent temperature boundary condition at one of the vertical sidewalls of an enclosure to enhance the natural convection heat transfer. They also found the existence of a resonance frequency. Later, in Chung et al. [32], the finite-wall effect within an enclosure which has a higher, time oscillatory temperature was numerically studied.

The above literature review clearly indicates that the non-uniform thermal boundary conditions, either spatial or temporary varying, will significantly alter the flow field and heat transfer in many applications. Especially, mixed convection heat transfer is very sensitive to the relative competition of the free and forced convection as well as to the assumed thermal boundary conditions. However, there is a lack of understanding of the mixed convection heat transfer with non-uniform thermal boundary conditions in a vertical channel, which is often met in practical applications. Thus, the present study is devoted to explore the aiding mixed convective heat transfer in a vertical channel with a finite heated section on one of the flat walls. In particular, the wall temperature is linearly varying along the axial coordinate. The governing equations associated with the boundary conditions are numerically solved. The aim of present study is to show how the governing variables affect the velocity and temperature fields, in turn, the heat transfer characteristics. Finally, according to the results, an excellent correlation which can accurately and easily estimate the average Nusselt number within the investigated parameters' ranges is proposed.

2. Analysis

Fig. 1 schematically shows the two-dimensional physical system and the coordinates for the mixed convection in a channel. A vertical parallel channel consists of two infinite plates with channel spacing b. A finite section $(0 \leqslant x \leqslant \ell)$ of the left wall is kept at non-uniform temperature which is higher than the inlet temperature. The rest of the left wall and the whole right wall are thermally insulated. A fully developed, forced flow enters the channel at temperature T_e in the far upstream. Since the flow considered here is slow, viscous dissipation is negligible. The plate spacing b and average inlet velocity $\overline{u_e}$ are used to non-dimensionalize the momentum and continuity governing equations and boundary conditions. Temperature difference between the channel inlet temperature T_e and the mean temperature of the heated section T_m is used to non-dimensionalize the energy equation and thermal boundary conditions. Thus, dimensionless governing equations for the steady two-dimensional, mixed convection for a Boussinesqs' flow through a vertical channel are

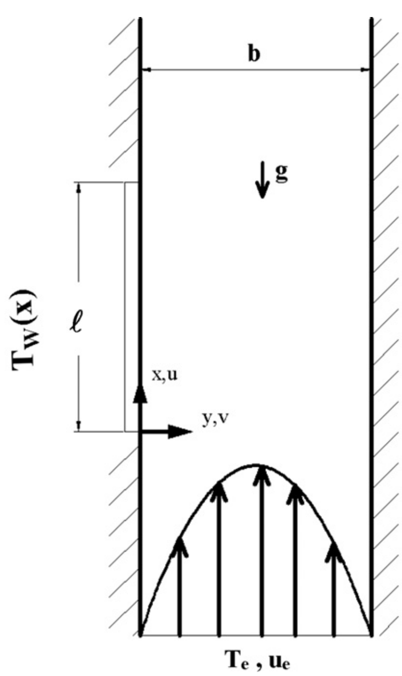

Fig. 1. Schematic diagram of physical system with aiding buoyancy.

Continuity equation:

$$\nabla \cdot \vec{V} = 0 \tag{1}$$

Momentum equation:

$$(\vec{V} \cdot \nabla)\vec{V} = -\nabla P + \frac{1}{Re}\nabla^2\vec{V} + \frac{Gr}{Re^2}\theta\vec{i} \tag{2}$$

Energy equation:

$$(\vec{V} \cdot \nabla)\theta = \frac{1}{Re \cdot Pr}\nabla^2\theta \tag{3}$$

where $\vec{V}$ is the velocity vector $U\vec{i} + V\vec{j}$ and $\vec{i}, \vec{j}$ are the unit vector in X and Y direction, respectively. The associated boundary conditions are

$$\begin{aligned}
&U = 6(Y - Y^2),\quad V = 0,\quad \theta = 0 \quad \text{at}\, X \to -\infty\\
&\frac{\partial U}{\partial X} = \frac{\partial V}{\partial X} = \frac{\partial \theta}{\partial X} = 0 \quad \text{at}\, X \to \infty\\
&\theta = \theta_1 + 2X(1 - \theta_1)/L,\quad U = 0,\quad V = 0 \quad \text{at}\, Y = 0,\quad 0 \leqslant X \leqslant L\\
&\frac{\partial \theta}{\partial Y} = 0,\quad U = 0,\quad V = 0 \quad \text{at}\, Y = 0,\quad X \leqq 0 \,\text{or}\, X \geqq L\\
&\frac{\partial \theta}{\partial Y} = 0,\quad U = 0,\quad V = 0 \quad \text{at}\, Y = 1
\end{aligned} \tag{4}$$

The dimensionless velocities U and V are zero on the solid boundaries. It is noted that the linearly varying temperature distribution is controlled by θ_1 which is the dimensionless temperature at $X = 0$ and $Y = 0$. The values of θ at the lower and upper ends of the wall section are θ_1 and $2 - \theta_1$, respectively. Accordingly, the temperature of this section increases with increasing X only when $\theta_1 < 1$. When $\theta_1 = 1$, the wall temperature is constant $(\theta = 1)$ over the heated section. When $\theta_1 > 1$, the wall temperature decreases from $\theta_1(X = 0)$ to $2 - \theta_1(X = L)$ with increasing X. Besides, θ is always unity at $X = L/2$ at left wall. The local Nusselt number of the heated section can be evaluated from equations:

$$Nu = \frac{hb}{k} = -\frac{\partial \theta}{\partial Y}\bigg|_{Y=0} \quad 0 \leqslant X \leqslant L \tag{5}$$

The dimensionless overall heat transfer rate is represented by averaged Nusselt number and defined as

$$\overline{Nu} = \frac{1}{L}\int_0^L Nu\,\mathrm{d}X \tag{6}$$

3. Solution method

A well-developed and verified program was modified to numerically solve the governing equations and associated boundary conditions. More details can be found in [33,34]. We briefly describe the numerical method. The projection method [35,36] is employed to numerically integrate the coupled momentum and continuity governing equations by two steps. First, a provisional velocity vector $\vec{V}^*$ is explicitly computed from previous velocity field $\vec{V}^n$ by ignoring the pressure gradient

$$\frac{\vec{V}^* - \vec{V}^n}{\Delta\tau} + \vec{V}^n \cdot \nabla \vec{V}^n - \frac{1}{Re}\nabla^2 V^n - \vec{B} = 0 \tag{7}$$

where $\vec{V}^n \nabla \cdot \vec{V}^n$ denotes the convective term, $\vec{B}$ the buoyancy force, and $\Delta\tau$ the artificial time step. Then, $\vec{V}^*$ is corrected by including the pressure effect and by enforcing the mass conservation at next step $n+1$,

$$\frac{\vec{V}^{n+1} - \vec{V}^*}{\Delta\tau} + \nabla P^{n+1} = 0 \tag{8}$$

and

$$\nabla \cdot \vec{V}^{n+1} = 0 \tag{9}$$

Substituting Eq. (8) into Eq. (9) yields the pressure Poisson equation

$$\nabla^2 P^{n+1} = \frac{1}{\Delta\tau}\nabla \vec{V}^* \tag{10}$$

Once we solved the pressure Poisson equation for P^{n+1}, we substitute it into Eq. (8) and explicitly calculate $\vec{V}^{n+1}$. Central difference is used to approximate all the derivatives except the convective terms when discretizing the above equations. To enhance numerical stability and accuracy, a third-order upwind scheme [37] is employed to discrete these convective terms. The power-law scheme [38] was used to discrete the energy equation with the time derivative treated implicitly. By using the Conjugated Gradient Squared method [39] to solve the resulting finite-difference equation system, the temperature can be quickly calculated to a very high accuracy. The flow is considered to be steady if the relative error of consecutive iteration for U, V and θ is less than 10^{-5} and overall energy balance is within 0.1%.

This program is originally written to numerically integrate the transient governing equations when the temporal dynamics of U, V, and θ are desired. Since we emphasize the steady thermal and flow characteristics varied with various governing parameters, only the steady results are

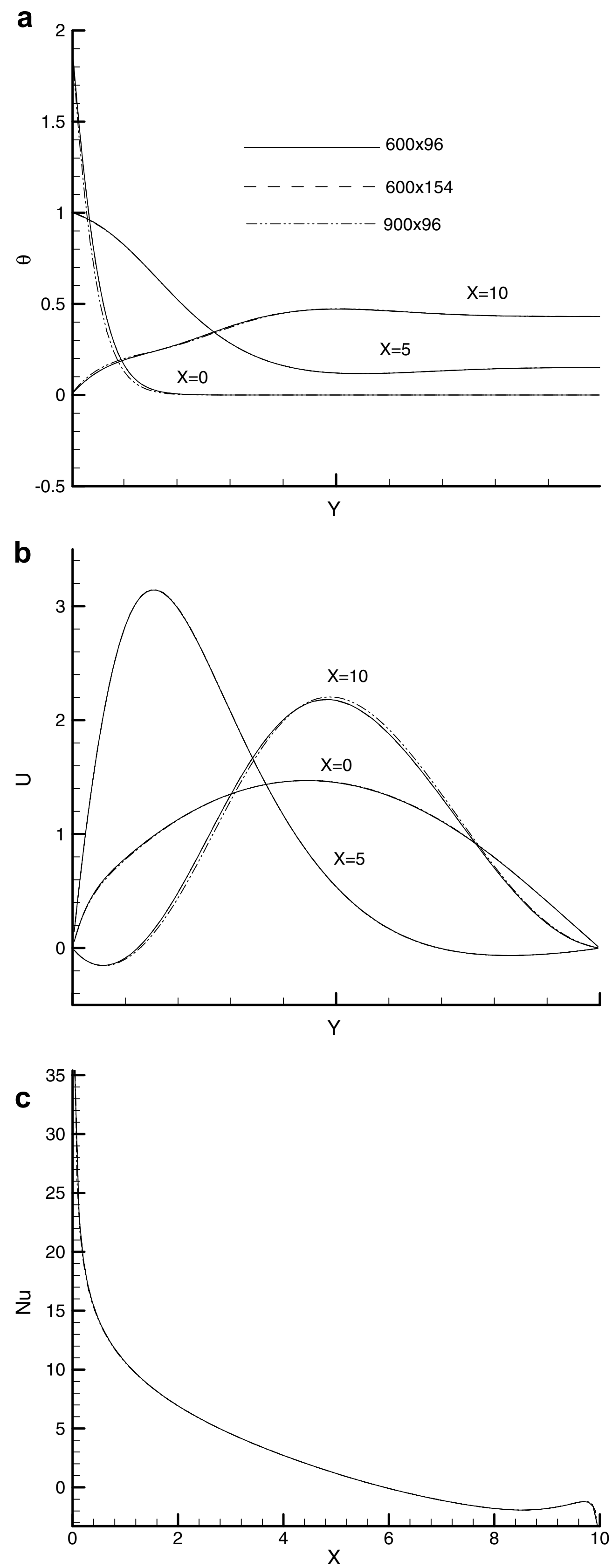

Fig. 2. Comparisons of (a) temperature, (b) velocity U and (c) local Nusselt number with various gridlines with $Re = 100$, $Gr = 4 \times 10^4$ and $\theta_1 = 2$.

presented in this work. In order to ensure the obtained results being grid-independent, computations were carried out with three gridlines systems, i.e., 600×96, 600×154 and 900×96, with $Re = 100$, $Gr = 4 \times 10^4$ and $\theta_1 = 2$ which is believed that the most complicated phenomena occurs. Some selected results are shown in Fig. 2. Excellent agreements are observed for local U and θ profiles at $X = 0$, 5 and 10. Three local Nu distributions are collapsed together indicating the grid-independent heat transfer rate. Additionally, the average Nusselt numbers are 3.12549, 3.12433 and 3.12766 for the three gridlines systems, respectively. These evidences strongly support that the adopted program is grid-independent. Therefore, 600×96 gridlines system is suitable and used throughout the present work.

4. Results and discussion

The foregoing problem formulation indicates that the steady mixed convection in a vertical channel with varying wall temperature is governed by five non-dimensional parameters: Reynolds number Re, Grashof number Gr, Prandtl number Pr, length of heated section L and the temperature at the beginning of the heated section ($X = 0$) θ_1. For the sake of computational load and to focus the effects of Re, Gr, and θ_1 on the heat transfer, air is used as the working fluid ($Pr = 0.71$) and $L = 10$ throughout this work. Computations will be carried out over wide ranges as Re from 100 to 500, Gr from 4×10^3 to 4×10^4 and $0 \leqq \theta_1 \leqq 2$. Local velocity U and θ along Y direction are plotted to illustrate in detailed flow and thermal characteristics. Particular attention is paid to the dependence of average Nusselt number on these important parameters. Finally, a correlation which can easily and accurately predict the average Nusselt number over the investigated range is proposed.

Effects of Gr, Re and θ_1 on the local velocity U and θ along Y direction at the entrance ($X = 0$), middle ($X = 5$) and exit ($X = 10$) of the heated section are examined first and shown in Fig. 3. In Fig. 3(a) and Fig. 3(b), Re and Gr are 500 and 4×10^3, respectively. Obviously, the heat transfer is dominated by the forced convection since there are a very strong inertia and a very weak buoyancy. Under this circumstance, no matter how θ_1 changes, the velocity profile is approaching to the fully developed, parabolic profile at the three different longitudinal positions, i.e. $X = 0$, 5 and 10. For the cases that the wall temperature linearly increases from $X = 0$ to $X = L$ i.e., $\theta_1 = 0$, the local temperature adjacent to the heated section gradually rises, too. For any axial cross section, the temperature is highest adjacent to the heated section then monotonically decreases with Y. There are several interesting features with $\theta_1 = 2$. First of all, it is noticed that the temperature distribution at $X = 0$ has a very sharp gradient adjacent to the heated section because the wall is hottest ($\theta_1 = 2$) and the fluid is cold. This fact implies a very high local heat transfer rate. Secondly, due to the better heat transfer around the entrance of heated section, more heat energy is transferred into the working fluid. Consequently, a higher temperature is observed at $X = 5$ for the case with $\theta_1 = 2$ than that with $\theta_1 = 0$. An increasing first then decreasing temperature profile is found with $\theta_1 = 2$ at $X = 10$. This particular temperature distribution has a positive temperature gradient in Y direction at the wall ($\frac{\partial\theta}{\partial Y}|_{Y=0} > 0$) means heat flux being transferred from the hotter fluid to the colder wall. Similar phenomena are observed in an infinite plate [7] and an enclosure with spatial varying wall temperature [16].

The results with $Re = 500$, $Gr = 4 \times 10^4$ are shown in Fig. 3(c) and (d). With a Gr 10-fold larger, the fluid beside the heated section is accelerated upward apparently. Velocity profile as well as the velocity peak shift toward the left wall ($Y = 0$). The temperature distributions are slightly varied as comparing Fig. 3(a) with 3(c).

Fig. 3(e) and (f) illustrates the temperature and velocity profiles with $Re = 100$ and $Gr = 4 \times 10^4$ in which inertia is weak and thermal buoyancy is relatively strong. Consequently, the velocity distributions may be significantly affected by the thermal buoyancy. For $\theta_1 = 0$, the local velocity U is similar to a parabolic profile at $X = 0$. Due to the strong enough buoyancy at $X = 5$, the velocity U reach a peak around $Y = 0.12$ then monotonically decreases with Y. At $X = 10$, the velocity neighbor to the heated section is so large that negative velocity is observed near $Y = 1$ to ensure the mass conservation. Therefore a recirculation is formed adjacent to $Y = 1$ in the downstream. For $\theta_1 = 2$, the velocity distribution at $X = 0$ deviates slightly from the parabolic profile. However, owing to the high wall temperature around $X = 0$, the velocity is dramatically distorted at $X = 5$ which is comparable to that at $X = 10$ with $\theta_1 = 0$. As the fluid flowing toward the downstream, the wall temperature decreases linearly, the energy of hotter fluid is transferred to the colder wall. As a result, negative velocity is found at $X = 10$ near to the left wall ($Y = 0$). Apparently, a recirculation is produced around the left wall.

Comparing Fig. 3(a), (c) and (e), it is found that the temperature distributions are limited nearby the left wall in Fig. 3(a) and (c), therefore the right wall is still kept at zero temperature. On the contrary in Fig. 3(e), the temperatures penetrate into the channel and the right wall's temperature is raised.

The local Nusselt numbers varied with different Gr, Re and θ_1 combination are displayed in Fig. 4. For $Re = 500$ and 4×10^3 in Fig. 4(a), forced convection is the main heat transfer mechanism. With $\theta_1 = 0$, Nu increases with X with a power of 0.6473; with $\theta_1 = 1$, i.e., isothermal surface, Nu decreases with X in a form, $Nu \propto X^{-0.378}$; while for $\theta_1 = 2$, $Nu \propto \ln X$. It is noted that with $\theta_1 = 2$, Nu becomes negative for $X > 6$. This fact implies that the heat is transferred from the fluid to the wall as explained in Fig. 3(a). There is no flow reversal at $X = 10$ as evident from Fig. 3(b) and Nu decreases from $X = 6$ to $X = 10$ monotonically.

Fig. 4(b) depicts the local Nusselt number distributions with $Re = 500$ and $Gr = 4 \times 10^4$. In spite of Gr being changed from 4×10^3 to 4×10^4, similar behaviors of Nu are

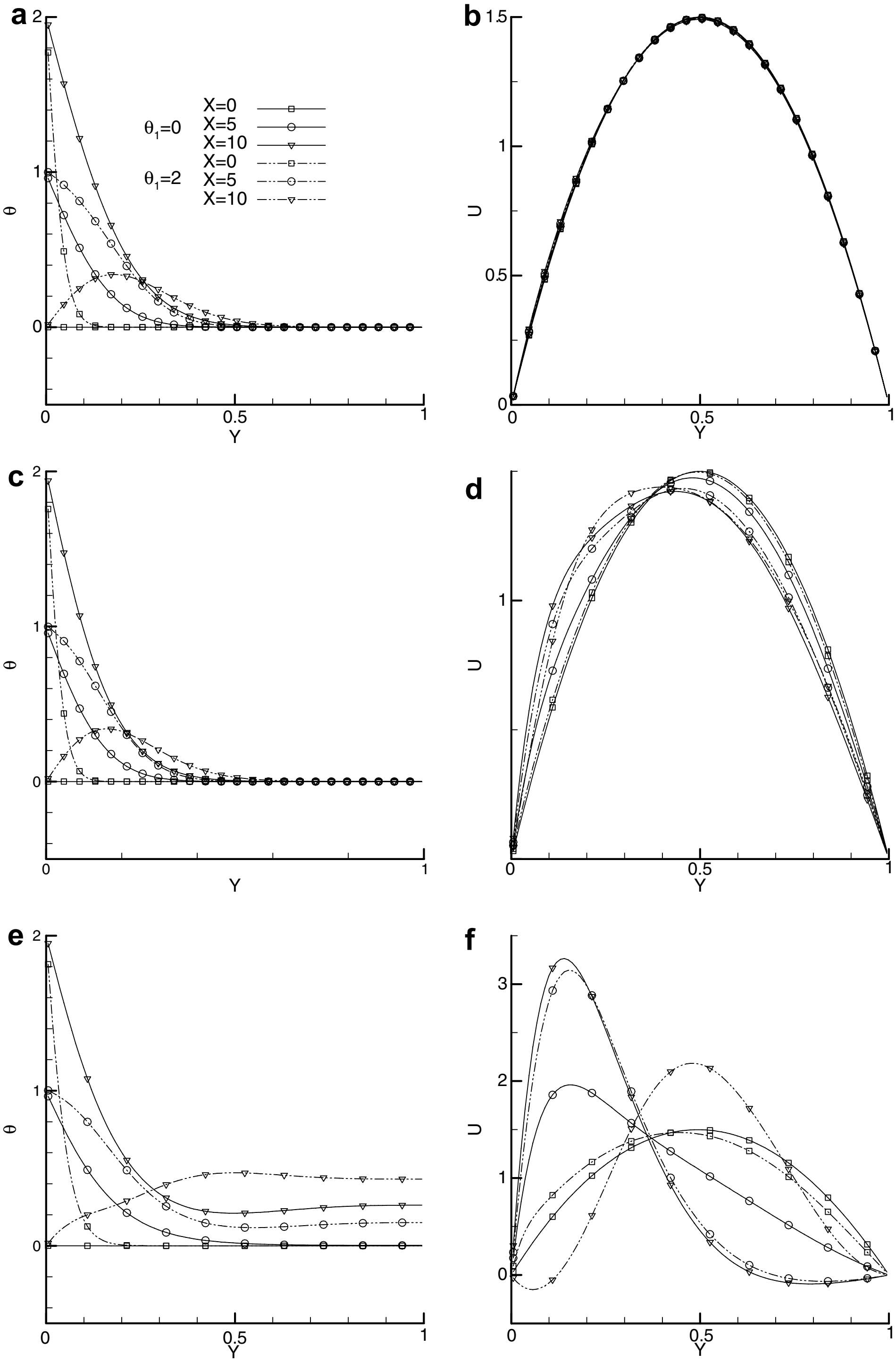

Fig. 3. Local velocity U, θ at entrance ($X = 0$), middle ($X = 5$) and exit ($X = 10$) of heated section with varied Re, Gr and θ_1.

observed for these two Grashof numbers. But after a close examination, Nu does increase with Gr because the reinforced aiding buoyancy force.

The local Nusselt number results with $Re = 100$ and $Gr = 4 \times 10^4$ are illustrated in Fig. 4(c). By comparing with Fig. 4(b), for both $\theta_1 = 0$ and $\theta_1 = 1$, similar trends are obtained except the lower Nu in Fig. 4(c). It is worthy to note that for $\theta_1 = 2$, at the end of the heated section, Nu first decreases, then slightly increases, finally abruptly drops which is different from the smoothly decreasing in Fig. 4(a) and (b). This unusual variation of Nu is resulted from the simultaneously action of the flow recirculation and the heat transferred from warmer fluid to the colder wall around $X = 10$.

After discussing the local distributions of U, θ_1 and Nu, we concern about the dimensionless average heat transfer

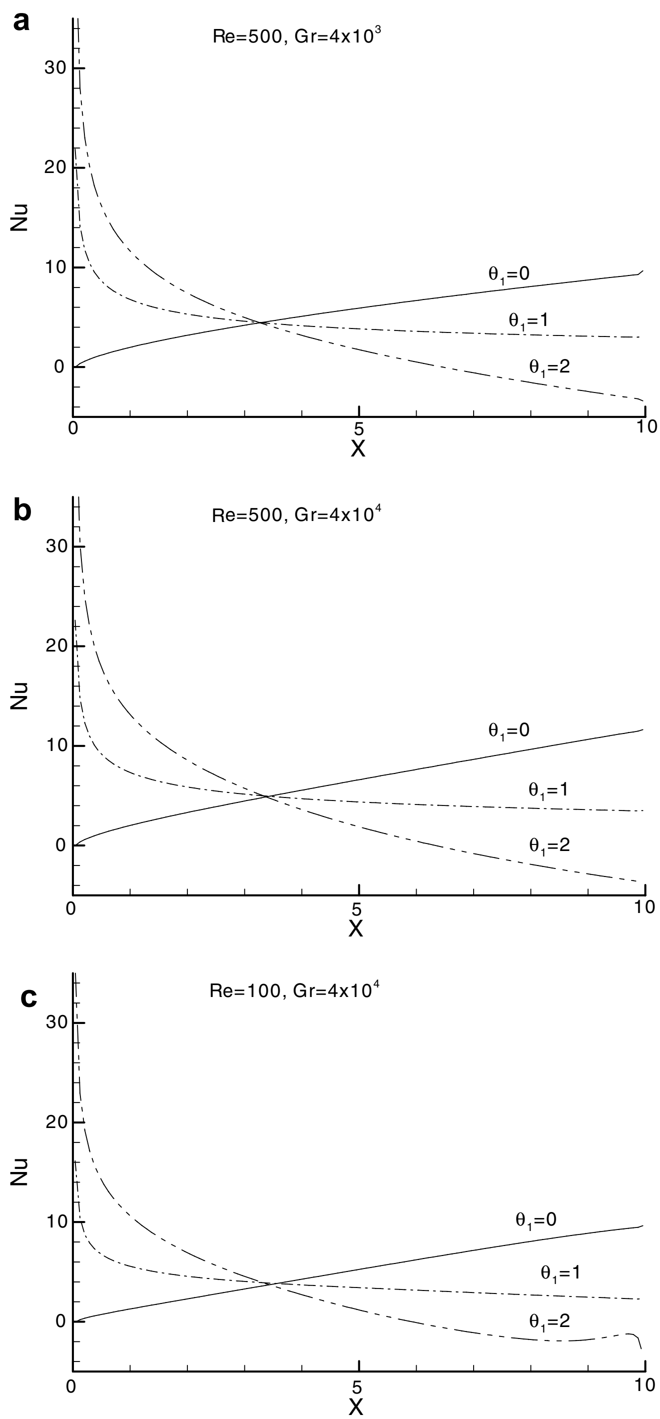

Fig. 4. Influences of Re, Gr and θ_1 on the local Nusselt numbers.

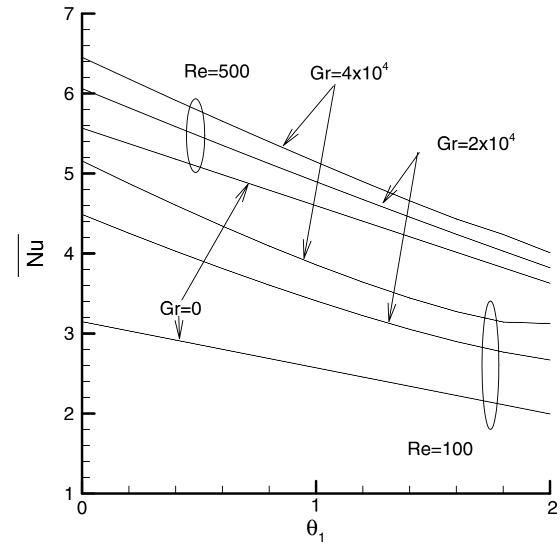

Fig. 5. Average Nusselt number dependence on θ_1 with various Gr and Re.

coefficient $\overline{Nu}$ varied with Gr, Re and θ_1. In Fig. 5, the abscissa is θ_1, representing the degree of wall temperature variation; Y axis is $\overline{Nu}$, representing the overall heat transfer rate. First of all, for any combination of Gr and Re, $\overline{Nu}$ always decreases with θ_1. It means that better heat transfer occurs when wall temperature linearly increases with X. Obviously with $Re = 100$, $Gr = 4 \times 10^4$ and $\theta_1 \geqq 1.8$, $\overline{Nu}$ is nearly the same because of the different Nu trend as shown in Fig. 4(c). For any θ_1, $\overline{Nu}$ increases with Re and Gr. This seems reasonable because increase of Re and/or Gr induces a higher local velocity adjacent to the heated section.

The monotonic variations of $\overline{Nu}$ depending on Gr, Re and θ_1 suggest to proposing a single correlation to describe the relationship between these dimensionless quantities. After a few try of different combinations, we obtain an empirical correlation as followed:

$$\overline{Nu} = \left\{ d + \frac{e}{[\exp(a + bRe^{0.5} + c\theta_1)]^{1.5}} \right\}^{-1} \quad \text{for any } Gr \tag{11}$$

where a, b, c, d and e are constants and related to Gr. Fig. 6 is plotted to demonstrate the parity plot of $\overline{Nu}_{\text{num}}$ and $\overline{Nu}_{\text{cor}}$ with $Gr = 4 \times 10^3$, 2×10^4 and 4×10^4. Re is ranged from 100 to 500 with increase 25 while θ_1 is ranged from 0 to 2 with increase 0.2. $\overline{Nu}_{\text{num}}$ and $\overline{Nu}_{\text{cor}}$ are $\overline{Nu}$ obtained from numerical simulation and from the proposed correlation, respectively. There are total 187 cases in each of Fig. 6(a)–(c) and are represented by the hollow squares. The solid lines represent the perfect correlation $\overline{Nu}_{\text{num}} = \overline{Nu}_{\text{cor}}$. Evidently, either the thermal buoyancy is negligible (i.e., forced convection, Fig. 6(a)) or not (i.e., mixed convection, Fig. 6(c)), accurate $\overline{Nu}$ can be easily obtained via the proposed correlation if Re and θ_1 are given.

Furthermore, we are going to extend the correlation to include the effects of Gr since we are aware that the coefficients a, b, c, d and e are functions of Gr only. To obtain enough data, computations were carried out for Gr ranged from 4×10^3 to 4×10^4 with increase 4×10^3. The ranges of Re and θ_1 are the same. Therefore, there are total 2046 points. The results are shown in Fig. 7 and indicate an excellent representation between $\overline{Nu}_{\text{num}}$ and $\overline{Nu}_{\text{cor}}$. The coefficients a, b, c, d and e are as followed:

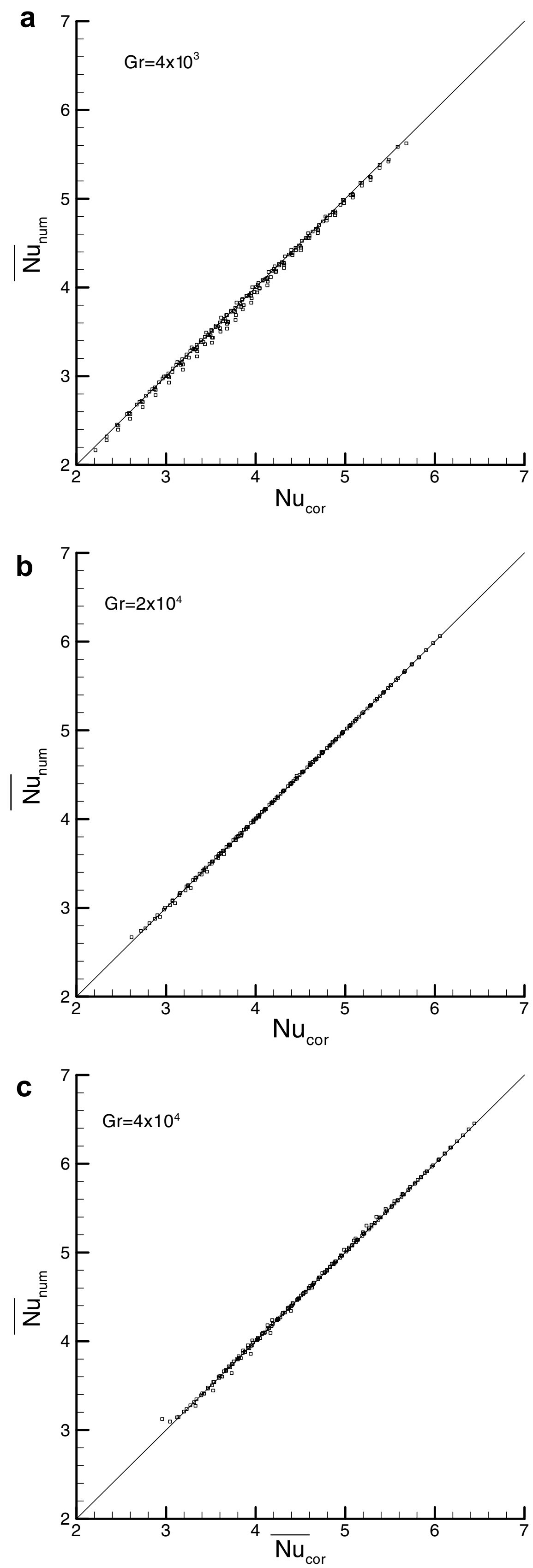

Fig. 6. Parity plot of $\overline{Nu}_{\mathrm{num}}$ vs. $\overline{Nu}_{\mathrm{cor}}$ for (a) $Gr = 4 \times 10^3$, (b) $Gr = 2 \times 10^4$, (c) $Gr = 4 \times 10^4$.

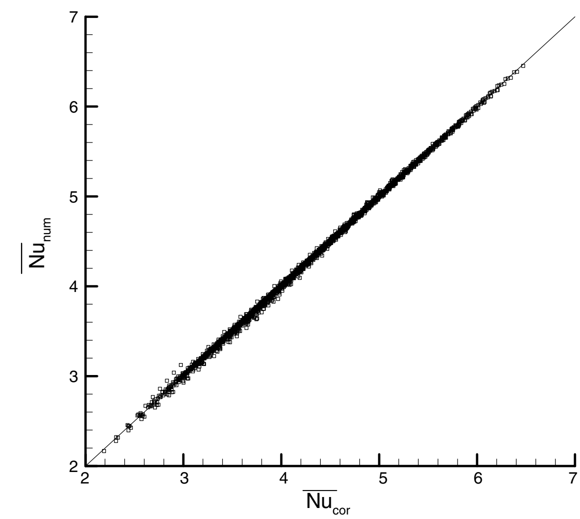

Fig. 7. Comparison of numerical simulated $\overline{Nu}$ results with correlation over the entire parameters' ranges.

$$
\begin{aligned}
a &= 0.8145 + 0.04455(\ln Gr)^2 \\
b &= 0.01562 + 0.0266\mathrm{e}^{(-Gr/124.44)} \\
c &= -0.02657 + 0.004898\mathrm{e}^{(-Gr/129.61)} \\
d &= (0.2989 - 0.005524Gr^{0.5})^2 \\
e &= 1.1205 + 0.1404Gr^{0.2184}
\end{aligned}
\tag{12}
$$

It is emphasized again that the most used isothermal boundary condition can be included in the present study by setting $\theta_1 = 1$. Therefore, the proposed correlation equation (11) with the coefficients Eq. (12) is also applicable to the isothermal surface as well.

5. Concluding remarks

Through a detailed numerical simulation, the laminar mixed convective heat transfer in a vertical channel with a finite section of linearly varying wall temperature on the left channel wall is investigated. Computations have been carried out over wide ranges of the governing parameters. The results can be briefly summarized as follows:

1. The presence of linearly varying wall temperature significantly changes the local velocity U, temperature θ, local Nusselt number Nu and, consequently, the average Nusselt number $\overline{Nu}$;
2. $\overline{Nu}$ increases with Gr and Re, but decreases with the assigned wall temperature at $X = 0$, θ_1;
3. An excellent correlation is proposed for $\overline{Nu}$ with the wide ranges of investigated parameters, i.e., Re from 100 to 500, Gr from 4×10^3 to 4×10^4 and θ_1 from 0 to 2.

Acknowledgement

The financial support of this study by the Engineering Division of National Science Council, ROC, through the contract NSC 93-2212-E-150-015 is greatly appreciated.

References

[1] F.P. Incropera, Buoyancy effects in double-diffusive mixed convection flows, in: C.L. Tein, V.P. Carey, J.K. Ferrel (Eds.), Proc. 8th Int. Heat Transfer Conf., vol. 1, 1986, pp. 121–130.

[2] W. Aung, Mixed convection in internal flow, in: S. Kakac, R.K. Shah, W. Aung (Eds.), Handbook of Single-Phase Convective Heat Transfer, Wiley, New York, 1987 (Chapter 15).

[3] B. Gebhart, Y. Jaluria, R.L. Mahajan, Sammarkia, Buoyancy-Induced Flows and Transport, Hemisphere, Washington, DC, 1988 (Chapter 10).

[4] W. Kays, A.L. London, Compact Heat Exchanger, third ed., McGraw-Hill, New York, 1993.

[5] D.Y. Lee, S.J. Park, S.T. Ro, Heat transfer in the thermally developing region of a laminar oscillating pipe flow, Cryogenics 38 (1998) 585–594.

[6] H.Y. Kim, H.C. Kim, V.V. Levdanskym, V.G. Leitsina, J. Smolik, Chemical deposition of substance from gas phase in nonisothermal channels, Int. J. Heat Mass Transfer 43 (2000) 3877–3882.

[7] L.N. Tao, On combined free and forced convection in channels, ASME J. Heat Transfer 82 (1960) 233–238.

[8] J. Quintiere, W.K. Mueller, An analysis of laminar free and forced convection between finite vertical parallel plates, ASME J. Heat Transfer 95 (1973) 53–59.

[9] S. Habchi, S. Acharya, Laminar mixed convection in a symmetrically or asymmetrically heated vertical channel, Numer. Heat Transfer 9 (1986) 605–618.

[10] W. Aung, G. Worku, Developing flow and flow reversal in a vertical channel with asymmetric wall temperature, ASME J. Heat Transfer 108 (1986) 299–304.

[11] L.C. Chow, S.R. Husain, A. Campo, Effects of free convection and axial conduction on forced convection heat transfer inside a vertical channel at low Peclet numbers, ASME J. Heat Transfer 106 (1984) 297–303.

[12] S.L. Yao, Free and forced convection in the entry region of a heated vertical channel, Int. J. Heat Mass Transfer 26 (1983) 65–72.

[13] T. Cebeci, A.A. Khattab, R. LaMont, Combined natural and forced convection in vertical ducts, in: U. Grigull, E. Hahne, K. Stephan, J. Straub (Eds.), Proc. 7th Int. Heat Transfer Conf., vol. 3, 1982, pp. 419–424.

[14] W. Aung, G. Worku, Theory of fully developed combined convection including flow reversal, ASME J. Heat Transfer 108 (1986) 485–488.

[15] A.S. Lavine, Analysis of fully developed opposing mixed convection between inclined parallel plates, Warme- und Stoffubertragung 23 (1988) 249–257.

[16] D.B. Ingham, D.J. Keen, P.J. Heggs, Two dimensional combined convection in vertical parallel plate ducts, including situations of flow reversal, Int. J. Numer. Methods Eng. 26 (1988) 1645–1664.

[17] D.B. Ingham, D.J. Keen, P.J. Heggs, Flows in vertical channels with asymmetric wall temperature and including situations where reversal flows occur, ASME J. Heat Transfer 110 (1988) 910–917.

[18] W.M. Kays, M.E. Crawford, Convective Heat and Mass Transfer, McGraw-Hill, New York, 1980.

[19] F.S. Ibrahim, I.A. Hassanien, Local nonsimilarity solutions for mixed convection boundary layer flow of a micropolar fluid on horizontal flat plates with variable surface temperature, Appl. Math. Comp. 122 (2001) 133–153.

[20] C.I. Hung, C.H. Chen, C.B. Chen, Non-Darcy free convection along a nonisothermal vertical surface in a thermally stratified porous medium, Int. J. Eng. Sci. 37 (1999) 477–495.

[21] C.Y. Cheng, An integral approach for hydromagnetic natural convection heat and mass transfer from vertical surfaces with power-law variation in wall temperature and concentration in porous media, Int. Comm. Heat Mass Transfer 32 (2005) 204–213.

[22] M. Ali, F. Al-Yousef, Laminar mixed convection boundary layers induced by a linearly stretching permeable surface, Int. J. Heat Mass Transfer 45 (2002) 4241–4250.

[23] E.M. Abo-Eldahab, M.A.E. Aziz, Viscous dissipation and Joule heating effects on MHD-free convection from a vertical plate with power-law variation in surface temperature in the presence of Hall and ion-slip currents, Appl. Math. Modell. 29 (2005) 579–595.

[24] M. Kumari, G. Nath, Mixed convection boundary layer flow over a thin vertical cylinder with localized injection/suction and cooling/heating, Int. J. Heat Mass Transfer 47 (2004) 969–976.

[25] E. Ramos, B.D. Storey, F. Sierra, R.A. Zuniga, A. Avramenko, Temperature distribution in an oscillatory flow with a sinusoidal wall temperature, In. J. Heat Mass Transfer 47 (2004) 4929–4938.

[26] J. Hernandez, B. Zamora, Effects of variable properties and non-uniform heating on natural convection flows in vertical channels, In. J. Heat Mass Transfer 48 (2005) 793–807.

[27] N.H. Saeid, Y. Yaacob, Natural convection in a square cavity with spatial side-wall temperature variation, Numer. Heat Transfer Part A 49 (2006) 683–697.

[28] Y.H. Dong, Xi.Y. Lu, Large eddy simulation of a thermally stratified turbulent channel flow with temperature oscillation on the wall, Int. J. Heat Mass Transfer 47 (2004) 2109–2122.

[29] A. Barletta, E. Zanchini, Time-periodic laminar mixed convection in an inclined channel, Int. J. Heat Mass Transfer 46 (2003) 551–563.

[30] M.S. Malashetty, D. Basavaraja, Effect of thermal modulation on the onset of double diffusive convection in a horizontal fluid layer, Int. J. Thermal Sci. 44 (2005) 323–332.

[31] H.S. Kwak, K. Kuwahara, J.M. Hyun, Resonant enhancement of natural convection heat transfer in a square enclosure, In. J. Heat Mass Transfer 41 (1998) 2837–2846.

[32] K.H. Chung, H.S. Kwak, J.M. Hyun, Finite-wall effect on buoyant convection in an enclosure with pulsating exterior surface temperature, In. J. Heat Mass Transfer 44 (2001) 721–732.

[33] T.F. Lin, T.S. Chang, Y.F. Chen, Development of oscillatory asymmetric recirculating flow in transient laminar opposing mixed convection in a symmetrically heated vertical channel, ASME J. Heat Transfer 115 (1993) 342–352.

[34] T.S. Chang, Y.H. Shiau, Flow pulsation and baffle's effects on the opposing mixed convection in a vertical channel, Int. J. Heat Mass Transfer 48 (2005) 4190–4204.

[35] A.J. Chorin, Numerical solution of the Navier–Stokes equation, Math. Comput. 22 (1968) 745–762.

[36] R. Temam, On an approximation solution of the Navier–Stokes equation by the method of fraction step: Part 1, Arch. Ration. Math. Anal. 32 (1968) 135–153.

[37] T. Kawamura, H. Takami, K. Kawahara, New-higher-order up-wind scheme for impressible Navier–Stokes equations, in: Proc. 9th Int. Conf. Numer. Math. Fluid Dynm, Springer-Verlag, 1985, pp. 291–295.

[38] S.V. Patankar, Numerical Heat Transfer and Fluid Flow, McGraw-Hill, New York, 1980.

[39] P. Sonneveld, CGS, a fast Lanczos-type solver for non symmetric linear systems, SIAM J. Sci. Stat. Comput. 10 (1989) 36–52.